

Degradation of Well Cements Exposed to Carbonated Brine

Andrew Duguid, Princeton University
Mileva Radonjic, Princeton University
George Scherer, Princeton University

Abstract

With increased attention on how people affect the climate, interest has grown in the anthropogenic emissions of greenhouse gases such as carbon dioxide. Subsurface carbon sequestration in abandoned petroleum fields may represent a chance to reduce CO₂ emissions. In order to understand how CO₂ may escape from the storage formation back to the atmosphere through abandoned wells, a set of four experiments was conducted. The experiments looked at how well cements reacted to carbonated brines at 20° and 50°C at pH 2.4 and 3.7. The results showed severe degradation to samples made from Class H well cement. The degradation occurred over the course of 31 days.

1. Introduction

The increased focus on how people affect the climate has spurred a growing interest in the anthropogenic emissions of greenhouse gases such as carbon dioxide. The annual emissions of CO₂ in 2001 were 6.5 GT/year [Energy Information Administration, 2003]. Greenhouse gases act to warm the globe by trapping energy from the sun in the earth's atmosphere. Global warming may be slowed if emissions of greenhouse gases are reduced. One possible way to reduce CO₂ emissions is to capture CO₂ at large point sources such as power plants and sequester it so it cannot reach the atmosphere. A possible method of disposal for the CO₂ is geologic sequestration, which is simply injection into the earth's subsurface. One plan is to inject CO₂ into depleted oil and gas fields. Some sites are already experimenting with geologic sequestration; these include Weyburn, Saskatchewan, in Canada [Brown et al., 2001], and Sleipner in the North Sea [Statoil, 2000].

If subsurface carbon sequestration in abandoned oil and gas fields is adopted, it will be important to understand how CO₂ may escape from the storage formation back to the atmosphere. Abandoned petroleum wells represent one potential avenue for leakage. When a well is installed, a hole is drilled in the ground to the desired depth and a pipe called the casing is placed in the hole. Then the casing is cemented into place by forcing cement into the annular gap between the casing and the formation. The cement, called the primary, acts to protect the casing and ensure the integrity of the well. When a well is abandoned, it is plugged in several places, or in some instances from top to bottom, with cement [Smith, 1993]. Within an abandoned well there are several pathways for the CO₂ to take if it travels back to the surface. The CO₂ may migrate (A) between the primary cement and the well casing, (B) through the primary cement, (C) along the interfaces between the primary cement and the geologic formation, (D) through the cement plug, or (E) between the casing and the cement plug. Figure 1 shows a schematic representation of these pathways.

A series of four experiments was carried out to examine the behavior of a typical Class H well cement under carbon storage conditions. The cements were exposed to carbonated NaCl (brine) solutions at pH 2.4 and 3.7 at room temperature (20°C) and 50°C for 31 days.

2. Methods and Materials

Experiments were run at 20° and 50°C, corresponding roughly to the temperature of the earth at the surface and 1 km below the ground [Hitchon, 1996 and Bruant et al.]. The leaching solution consisted of a 0.5 M NaCl (brine) solution that was at either pH 2.4 or pH 3.7, both of which are likely pH conditions based on calculations using EQ3_6 Version 8. The brine was carbonated by bubbling CO₂ through it, which brought the pH to 3.7. The pH was further adjusted using HCl to lower it to pH 2.4. Each experiment was run for 31 days in a 1.8-L reaction vessel; one reactor was setup for each condition. A schematic of the experimental system is presented in Figure 2. The flow rates in the vessels were between 8.3 and 8.4 ml/min (flow velocity around 0.16 cm/min) for the room temperature experiments and 8.6 and 8.7 ml/min (0.17 cm/min) for the 50°C experiments. The residence time for reactors was 3.6 hours for the room temperature vessels, 3.4 hours for the 50°C-pH 2.4 reactor, and 3.5 hours for the 50°C-pH 3.7 reactor. The reactor vessels were made from graduated cylinders plugged with a two-hole stopper.

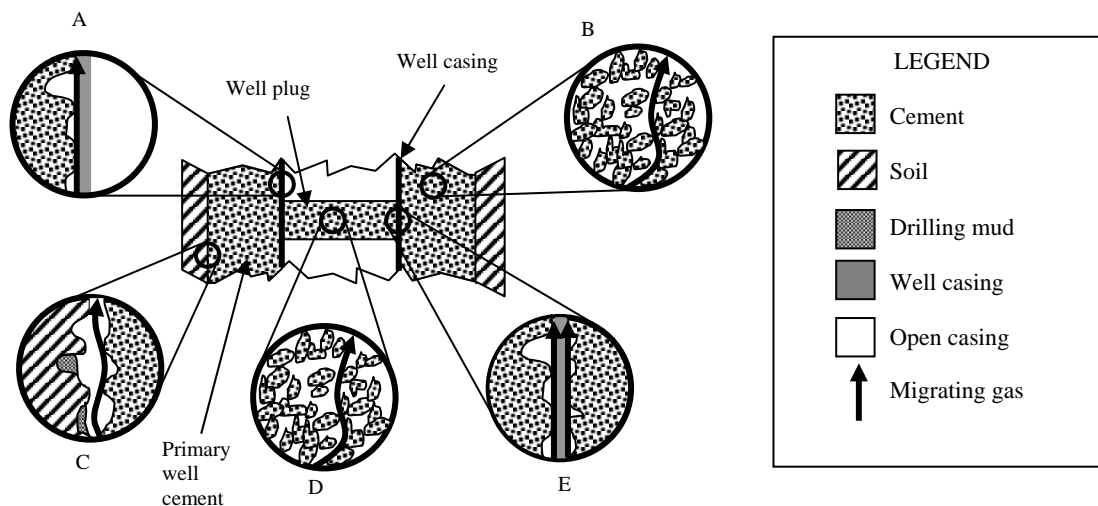


Figure 1 Potential leakage pathways within an abandoned well. (A) Flow through the annulus between the well cement and the well casing. (B) Gas migration through the well cement. (C) Short circuiting between the formation and the well cement. (D) Gas migration through the well bore plug. (E) Short circuiting between the well plug and the casing and the well cement and the casing.

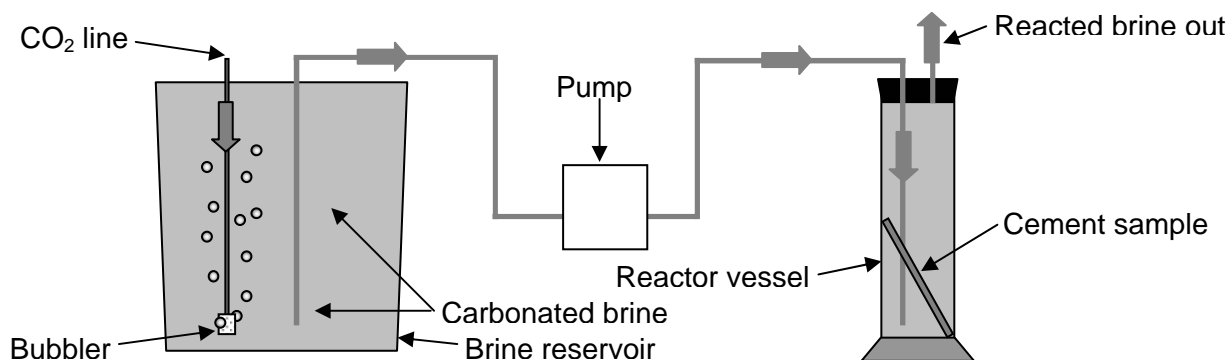


Figure 2 Flow-through reactor system.

The influent and effluent lines ran through the stopper. The influent line ran to within 2 cm of the bottom, forcing the influent flow to change directions and stir the system before exiting.

Effluent samples and pH measurements were taken twice a day for the first three days and then daily for the remainder of the experiment. Cement samples were taken throughout the experiment. The pH was measured at the influent using a Thermo Orion 230A pH meter to ensure it remained steady. The composition was measured for calcium, silicon, and magnesium using ICP-OES. Physical measurements of samples and the advance of different fronts within the samples were taken using an optical microscope with a digital camera. X-ray diffraction, XRD, was used to help identify crystalline phase and reaction products in the samples. EPMA analysis was used to look at calcium intensity in a line between the outer edge and the center of the samples.

The cylindrical samples were made out of Class H well cement (LaFarge Class H HSR) with a

W/C ratio of 0.38. This W/C ratio was suggested by Haliburton Services Company as being a typical well cement W/C ratio; this was also the W/C ratio used by Bruckdorfer [1986] and Onan [1984]. The samples were 12 months old at the time the experiments were started. Leading up to the experiment they were cured in uncarbonated brine at the same temperatures as the experiments, either 20° or 50°C. Storage in brine instead of a saturated calcium hydroxide solution is closer to the condition cement would see in a well. The dimensions of the samples were approximately 7.5 mm x 200 mm. The cement used to cast the samples was mixed according to API Recommended Practice 10B [1997]. Two samples were placed in each reactor vessel.

3. Discussion

Each of the samples degraded during the course of the experiment. Slices of the samples taken throughout the experiment show a series of rings formed and progressed inward. The samples that were reacted with an influent pH of 2.4 showed five different regions. The outermost region was an orange ring, followed by a brown ring, a white ring, a light gray ring, and a gray core. The samples that were reacted at influent pH 3.7 had the same pattern of rings with the exception that there was no orange ring; the brown ring was the outer ring. Figure 3 shows the ring pattern for the samples reacted at 50°C; the pattern was the same for those reacted at room temperature. Figures 4 and 5 show the progression of the rings over the course of the experiments for the samples that were reacted at 50°C. The orange and brown rings were soft to the touch and easily damaged. This caused the diameter of the sample to be reduced during the experiment. Each of the rings widened as the experiments progressed until it became the core; then it shrank away as it was replaced by the next ring. The rate of advance of the regions was calculated from plots of the diameter versus time by fitting a straight line to the data; see Figure 6. The samples that were reacted at 50°C and pH 2.4 generally showed the fastest rates of advance, varying between 0.0188 and 0.240 mm/day for the outside edge of the sample and the outside edge of the gray core. The only exception was that the rate of the gray core at 50°C and pH 3.7 was slightly faster than the rate for 50°C and pH 2.4. For all of the experiments the rates at 50°C were faster than the same pH experiments at room temperature. The rates of advance for the layers are given in Table I.

The effluent pH profiles over the 31 days show an initial increase to near pH 5 for the influent pH 3.7 reactors within the first day. Then there was a slow decline for the remainder of the experiment. The reactors that had a pH 2.4 influent jumped to an effluent pH of 2.8 for the room temperature experiment and 3.6 for the 50°C experiment. The pH of both reactors quickly (within a week) returned to within a tenth of a pH unit of the influent and remained there for the rest of the experiment. The initial increase of the 50°C reactors was always above that of the room temperature reactors. The influent pH was monitored and did not fluctuate more than a tenth of a pH unit during the course of the experiments. The pH profiles are shown in Figure 7A.

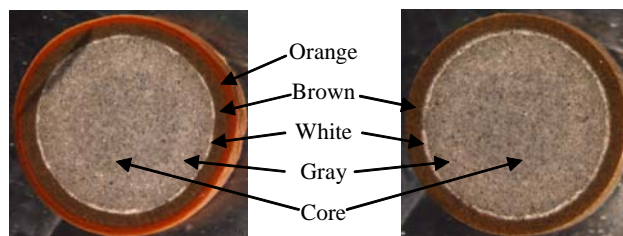


Figure 3 Reaction zones for 50°C samples run with influent pH 2.4 (left) and 3.7 (right).

The chemical composition of the effluent was investigated for Ca, Si, and Mg using ICP-OES. All of the chemical profiles show an initial jump in concentration from 0 mg/L to the maximum within the first few days and then a decline for the rest of the experiment. The pH 2.4-50°C reactor had the highest initial increase, and generally the ionic concentrations are higher than those of the other reactors throughout the experiment. The 50°C reactor for the pH 3.7 experiment showed a larger initial increase than did the pH 3.7 reactor at room temperature. Figure 7 shows the concentration profiles for the reactor effluents.

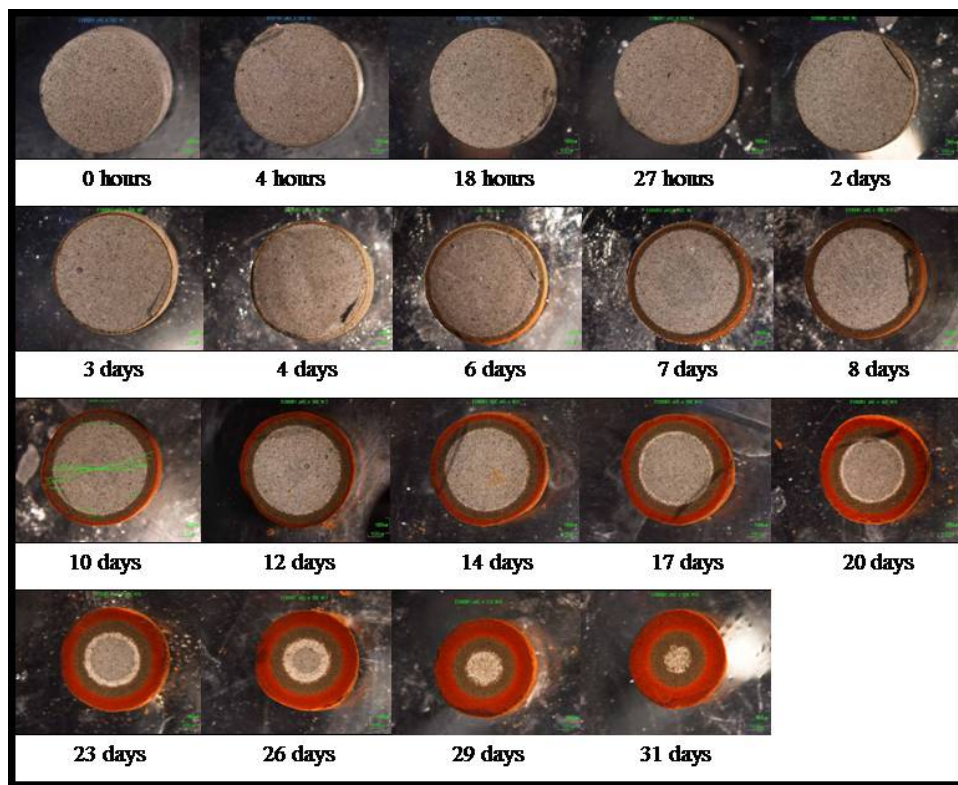


Figure 4 Progression of the reaction zones within the sample over the course of the experiment.

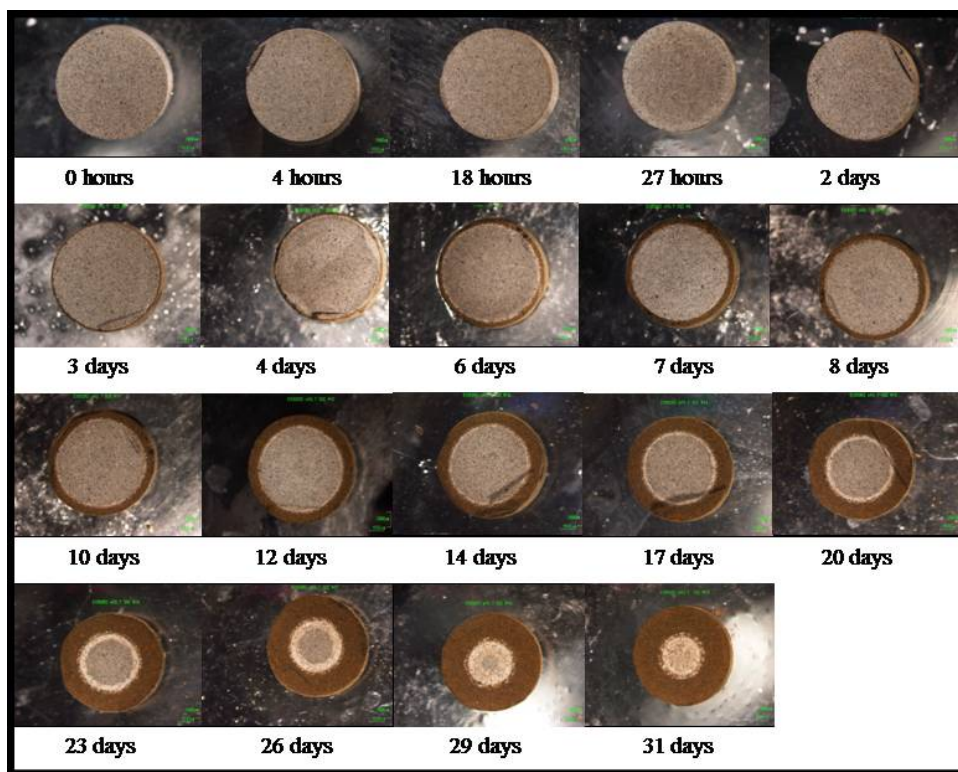


Figure 5 Progression of the reaction zones within the sample over the course of the experiment.

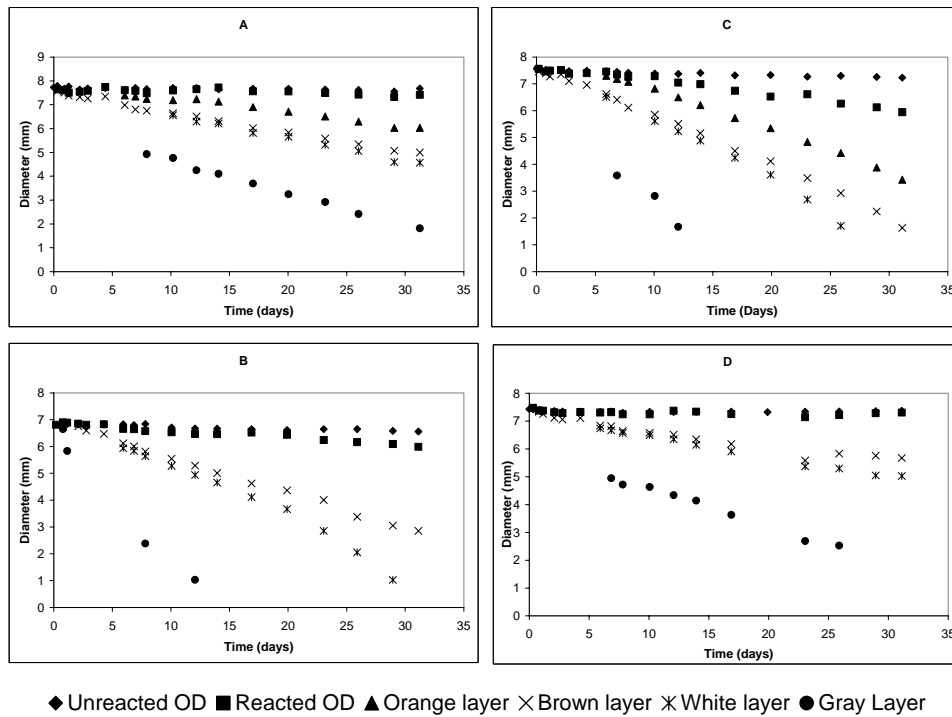


Figure 6 Plots showing the diameters of the reacted rings over the course of the experiment. The plots are (A) pH 2.4 at room temperature, (B) pH 3.7 at 50°C, (C) pH 2.4 at 50°C, and (D) pH 3.7 at room temperature.

Table I Rates of advance (mm/day) of the outer edge of reacted layers.

| Layer | pH 2.4 at 50°C | pH 2.4 at 20°C | pH 3.7 at 50°C | pH 3.7 at 20°C |
|----------------|----------------|----------------|----------------|----------------|
| Orange layer | 0.0254* | 0.0034* | None | None |
| Brown layer | 0.0758 | 0.0284 | 0.0136* | 0.0021* |
| White layer | 0.0923 | 0.0419 | 0.0668 | 0.028 |
| Gray layer | 0.117 | 0.0482 | 0.101 | 0.0361 |
| Dark gray core | 0.240 | 0.0677 | 0.244 | 0.0661 |

* Corresponds to the rate of change in the total radius (the outer edge) of the sample.

XRD was run on the layers of each sample after 31 days. At this point the sample that was reacted at pH 2.4 and 50°C had an orange layer, a brown layer, and a white core. The sample that was reacted at pH 3.7 and 50°C had a brown layer and a white core. The samples that were reacted at room temperature showed an orange layer, a brown layer, a white layer, a light gray layer, and a dark gray core. The pH 3.7 sample showed a brown layer, a white layer, a light gray layer, and a dark gray core. The analysis of the pH 2.4 samples indicated that the orange layer contained iron oxide. The brown layer contained brownmillerite ($\text{Ca}_2\text{AlFeO}_5$). The white layer/core contained three polymorphs of CaCO_3 , calcite, aragonite, and vaterite. The white layer also contained $\text{Ca}_2\text{AlFeO}_5$. The brown layer and white core in the pH 3.7-50°C sample contained the same phases as the white layer and brown core in the pH 2.4-50°C sample. The sample that was reacted at pH 2.4 and 20°C showed iron oxide in the orange layer, brownmillerite in the brown layer, calcite and brownmillerite in the white layer, calcite and brownmillerite in the light gray layer, and portlandite (CaOH), brownmillerite, and calcite in the dark gray core. The 20°C sample that was reacted at pH 3.7 had the same phases in the corresponding layers. Both unreacted cements showed portlandite and brownmillerite. The room temperature cement also showed a small calcite peak. Figure 8 presents the count spectra for the samples that were reacted at 50°C.

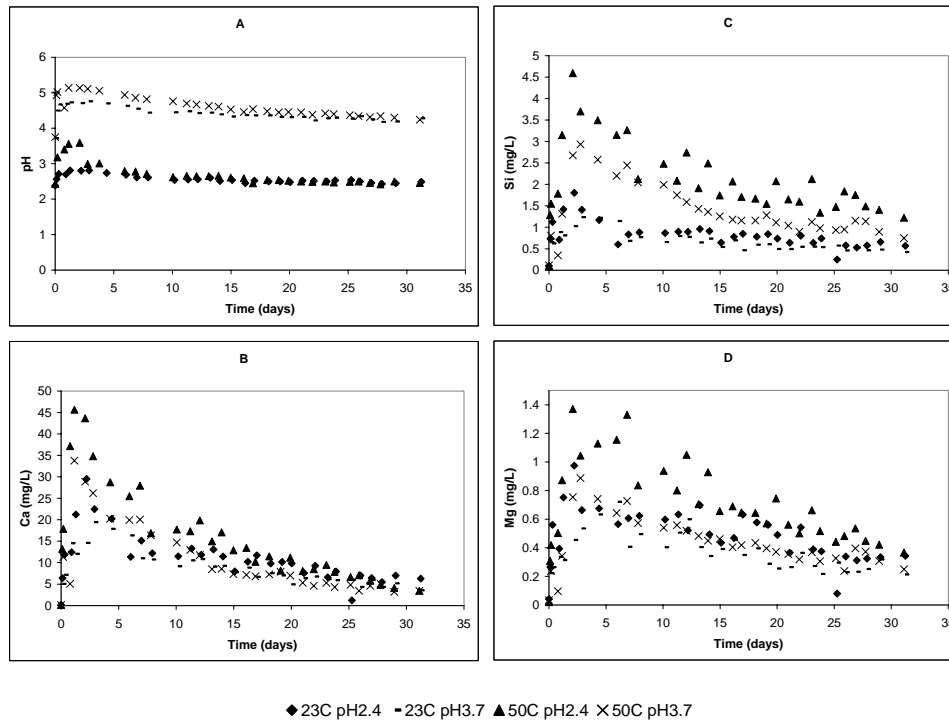


Figure 7 pH and chemical profiles over time for all reactors. The plots are (A) pH versus time, (B) calcium versus time, (C) silicon versus, and (D) magnesium versus time.

Table II summarizes the crystalline phases identified in the reacted samples. EMPA analysis was conducted on samples from each pH and temperature at the end of the experiment. The results of the analyses showed that the sample that was reacted at 20°C and pH 2.4 (Figure 9A) underwent an almost total depletion of calcium, near-zero intensity, in the orange and brown layers, 0 to 0.8 mm on the plot. The white layer (0.8 to 1.2 mm) showed a transition from almost no calcium to the maximum amount of calcium in the sample; the intensity went from near zero to between 30 and 35. The rest of the sample, from 1.2 to 3 mm, is the light gray layer. This layer exhibited some depletion of calcium between 2 and 3 mm. The dark gray core was not measured for this sample.

An X-ray map of the sample (pH2.4-20°C) revealing the calcium distribution is presented in Figure 10. Figure 9B shows the results for the cement that was reacted at 20°C-pH 3.7. This sample also showed a nearly complete depletion of calcium, near-zero intensity, in the brown layer (0 to 0.6 mm). The white layer (0.6 to 0.9 mm) had more calcium than any other layer in the sample with an intensity that reached 50. The light gray layer (0.9 to 2.2 mm) had an intensity between 10 and 20. The dark gray core showed more calcium than the light gray layer with an intensity between 20 and 30. The sample that was at 50°C-pH 2.4 (Figure 9C) also exhibited near-zero intensity in the orange and brown layers between 0 and 1.2 mm. The rest of the sample between 1.2 and 2 mm is the white layer. This layer had an intensity reaching around 50. The sample that was reacted at 50°C-pH 3.7 showed the same pattern as the one that was reacted at 50°C-pH 2.4. The brown layer (0-0.5 mm) had near-zero intensity and the white layer had an intensity reaching around 35. It is important to note that the sample diameters for these analyses do not match the sample diameters presented in the plots in Figure 6. The drying and polishing of the samples damaged the outer layers and caused some shrinkage of the samples.

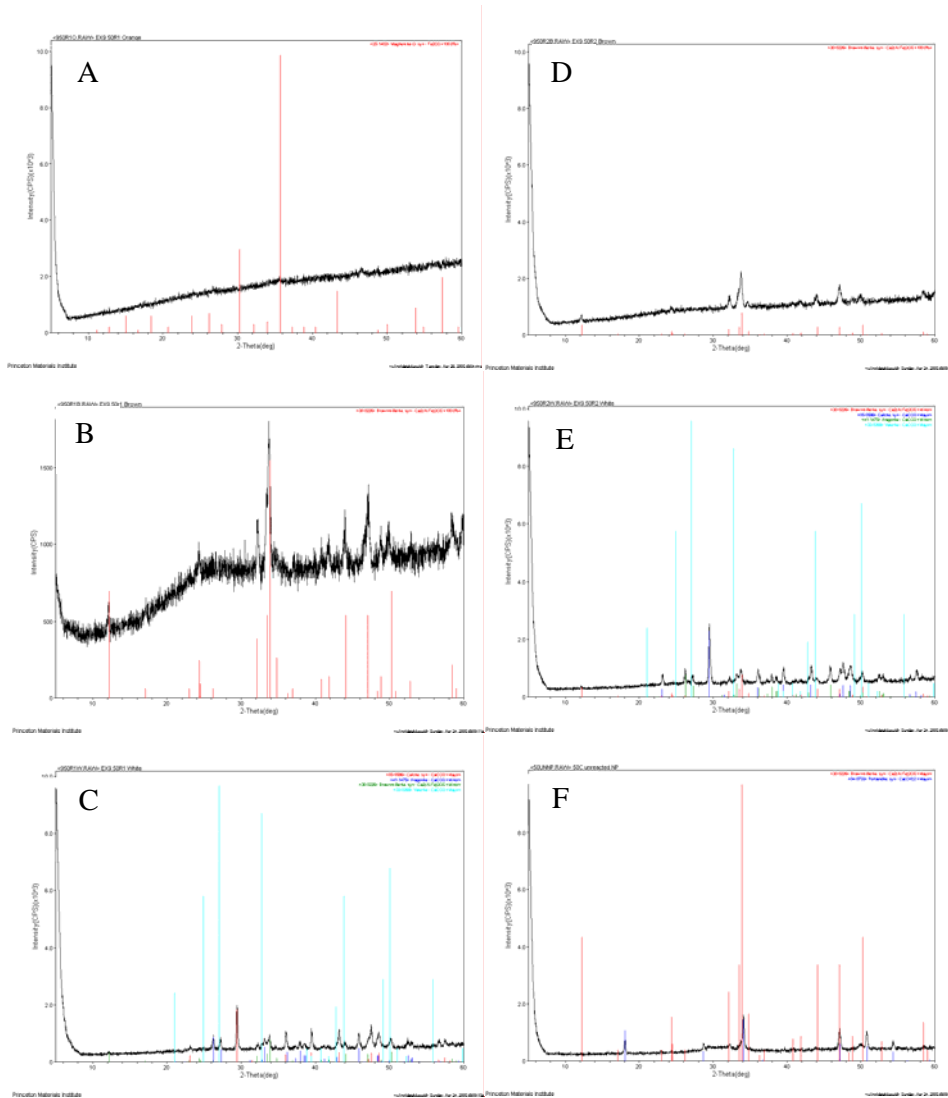


Figure 8 XRD results for neat paste reacted for 31 days at 50°C with influent pH 2.4. The plots are (A) pH 2.4 orange layer, (B) pH 2.4 brown layer, (C) pH 2.4 white core, (D) pH 3.7 brown layer, (E) pH 3.7 white core, and (F) unreacted cement paste.

Table II Crystalline phases identified in the reacted and unreacted cement samples.

| | pH 2.4 50°C | pH 3.7 50°C | pH 2.4 21°C | pH 3.7 21°C |
|--------------------|----------------------------------|----------------------------------|--|--|
| Orange layer | Iron oxide | No layer | Iron oxide | No layer |
| Brown layer | Brownmillerite | Brownmillerite | Brownmillerite | Brownmillerite |
| White layer / core | Calcite Aragonite Vaterite | Calcite Aragonite Vaterite | Calcite | Calcite |
| Light gray layer | No layer | No layer | Portlandite Calcite | Portlandite Calcite |
| Dark gray core | No layer | No layer | Portlandite Calcite Brownmillerite | Portlandite Calcite Brownmillerite |

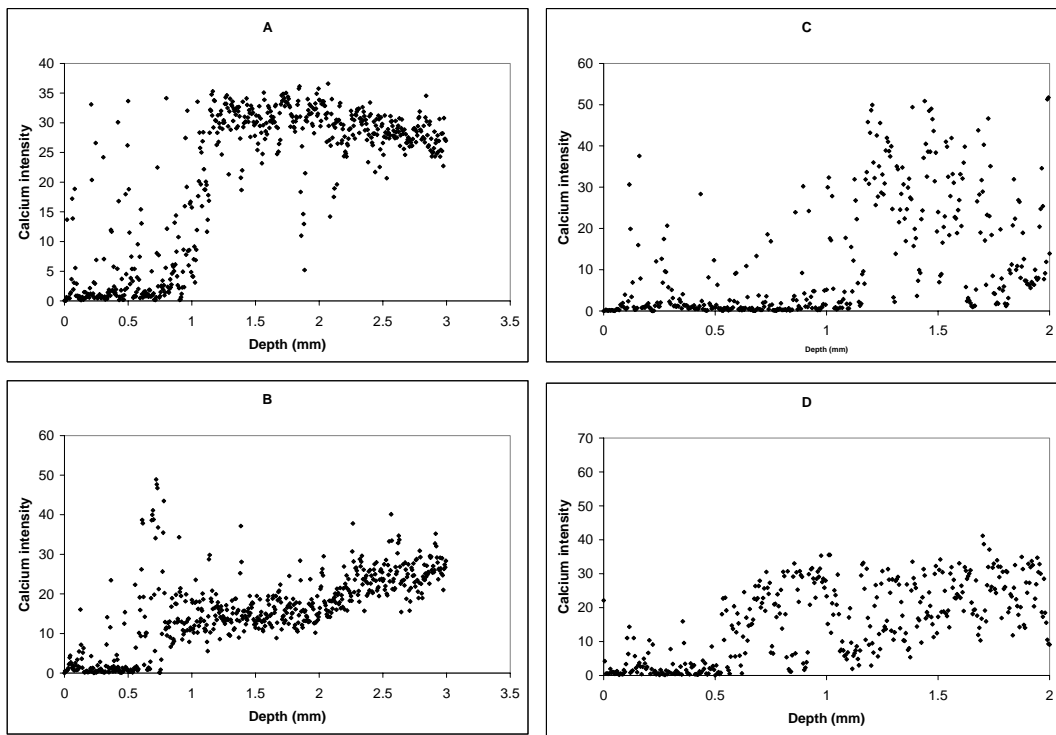


Figure 9 EMPA analyses of the reacted samples after 31 days of exposure showing calcium intensity between the outer edge (0 mm) and the center of the sample. The plots show (A) pH 2.4-20°C, (B) pH 3.7-20°C, (C) pH 2.4-50°C, and (D) pH 3.7-50°C.

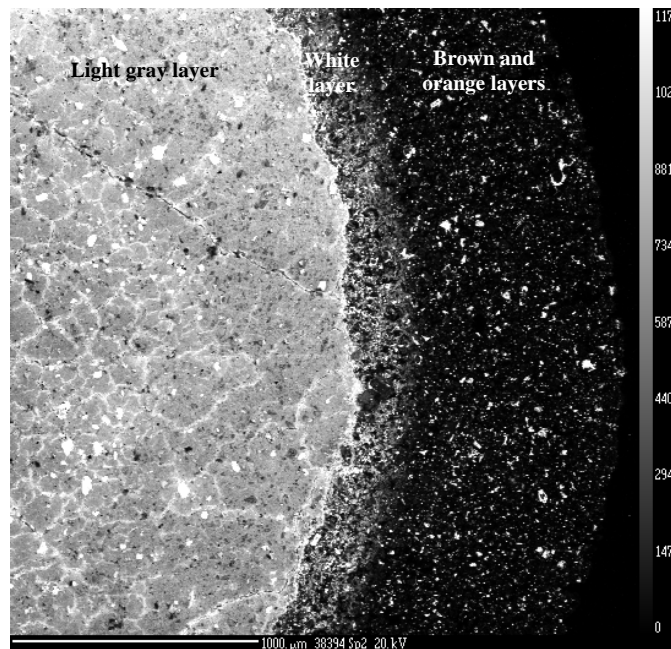


Figure 10 X-ray map showing calcium intensity for the sample that was reacted at pH 2.4-20°C. The concentration spectrum is a gray scale, with the highest concentrations in white and the lowest in black.

4. Discussion

The multi-ring pattern of degradation exhibited by each of the samples suggests that different phases within the samples are reacting at different speeds. Evidence for this is also found in the XRD spectra, where different layers have different crystalline phases. The formation of an orange layer only occurs in the samples that were reacted at pH 2.4. This is probably due to a change in the iron-containing cement phases. Brownmillerite ($\text{Ca}_2\text{AlFeO}_5$) is present in the unreacted cement and all of the reacted layers except for the orange layer. The dissolution of brownmillerite would release iron oxide phases and turn the layer from brown to orange. Other researchers have seen similar reaction layer formations. Andac and Glasser [1999] reacted a Portland cement that contained 10 percent fly ash in a carbonated system and found five reaction layers. The XRD data show degradation is taking place; no calcium hydroxide (CH) was found in the orange, brown, white, or light gray layer. Portlandite was found in the unreacted cement and in the dark gray core. If degradation was not occurring, one would expect to find portlandite, which normally makes up around 20 percent of a hydrated Portland cement throughout the sample [Glasser, 1993]. The XRD analysis also found that there was no calcium carbonate, a reaction product from the carbonation of both portlandite and calcium-silica-hydrate (C-S-H) [Thaulow et al., 2001], in the outer reacted layers, but there was calcium carbonate in the inner layers and the core. This means that the CH and C-S-H in the samples were reacting with the carbonated brine to form calcium carbonate and the calcium carbonate was then being destroyed. C-S-H is the main phase in hydrated cement paste; it is the glue that holds the cement together.

In general the reaction rings moved the fastest at pH 2.4 at 50°C, making this condition the most severe in terms of degradation. The 50°C reactions always occurred faster than their room temperature counterparts, and influent pH 2.4 reactions always occurred faster than influent pH 3.7 reactions at a given temperature. These results show that lower pH and higher temperature cause faster degradation and that the role of temperature has more effect on degradation rates than pH. Tables III and IV show the percent change in rate when going up in temperature (Table III) and down in pH (Table IV). The data show that change in temperature is more significant than change in pH with respect to rate increase.

Table III Percent change in rate when going from 20° to 50°C at a given pH.

| | Change in rate at pH 2.4 (%) | Change in rate at pH 3.7 (%) |
|------------------|------------------------------|------------------------------|
| Orange layer | 87 | No layer |
| Brown layer | 63 | 85 |
| White layer | 55 | 58 |
| Light gray layer | 59 | 64 |
| Dark gray core | 72 | 73 |

Table IV Percent change in rate when going from pH 3.7 to pH 2.4 at a given temperature.

| | Change in rate at 50°C (%) | Change in rate at 20°C (%) |
|------------------|----------------------------|----------------------------|
| Outside layer* | 47 | 37 |
| White layer | 28 | 33 |
| Light gray layer | 13 | 25 |
| Dark gray core | -1.5 | 2.4 |

* This designates a rate change between the outer edge of the orange sample at pH 2.4 and brown layer at pH 3.7.

Since the combination of low pH and high temperature is a likely sequestration condition, it may mean that cement in existing abandoned wells could be damaged by sequestration. The pH conditions used in these experiments are intended for a system in which the host rock will not buffer the local groundwater, a sandstone formation for example. If sequestration were to take place in a limestone or dolomite formation, the pH of the formation fluid would be higher and the degradation slower.

The rate of advance of the reaction rings appears to be linear. This contrasts with the results of Islam et al. [2004], who found that leaching occurred with the square root of time. The likely reason for the discrepancy is that the conditions of the two sets of experiments were not the same. Islam et al. used nitric acid in a batch reactor with a constant pH ranging between 4 and 7. It is possible their batch reactor allowed the reaction to approach equilibrium and slow the reaction over time. By using a continuously stirred flow-through reactor, the reactions in this set of experiments were kept far from equilibrium, which allowed the linear progression.

It is clear from the ICP analysis that calcium, silica, magnesium, and probably other components within the cement are being leached from the sample from the start of the experiments. There is a change in slope of the calcium concentration profiles between 7 and 10 days, which is approximately the same time that the white layer becomes visible. This may indicate that the white layer has a protective property. Further evidence of the protective property of the white layer can be seen by dividing the effluent concentration by the surface area of the light gray core. Dividing surface area removes the effect of the shrinking core from the data. The light gray core is used because the C-S-H at this point has not been totally degraded; it is still cement paste. The results of this show that the $[Ca^{2+}]/\text{area}$ data level out after the formation of the white layer, which means that the calcium leaching rate becomes constant. The leveling of these data also indicates that diffusion through the brown and/or orange layers does not control the degradation of the sample. Instead that rate of dissolution of the white layer controls the rate of degradation of the cement. If diffusion through the orange and/or brown layers were important, one would expect the values of the data to decrease with time. The formation of the calcium carbonate-containing white layer does not stop the degradation; it only slows the rate. Figure 11 shows plots of calcium concentration divided by surface area.

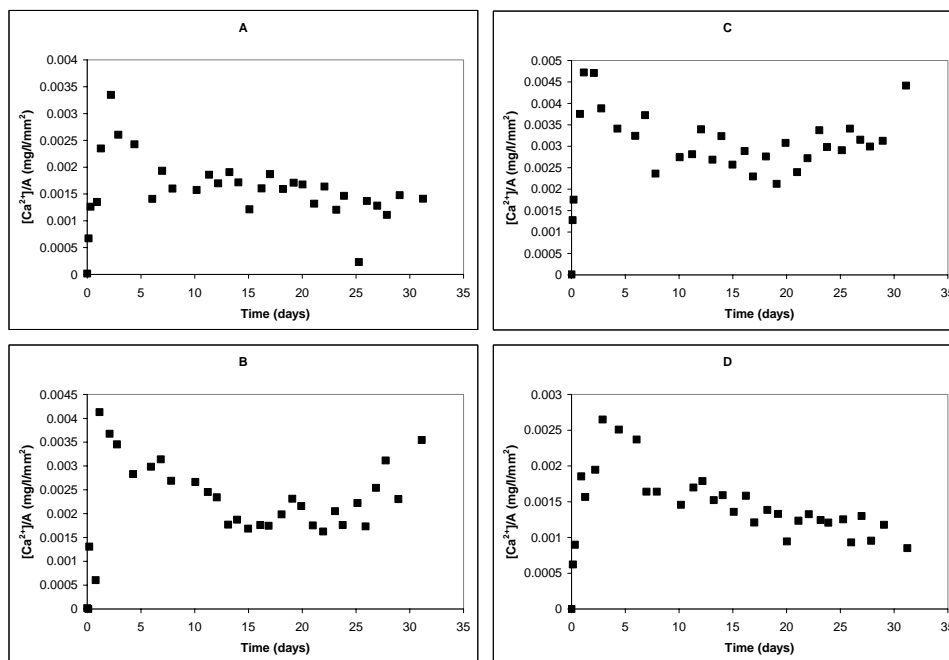


Figure 11 Effluent calcium concentration divided by sample surface area: (A) pH 2.4 at room temperature, (B) pH 3.7 at 50°C, (C) pH2.4 at 50°C, and (D) pH3.7 at room temperature.

The EPMA data give further evidence that the calcium-containing phases are being destroyed in the cement. All of the samples show severe calcium depletion in the outer layer or layers. The data show that the white layer is enriched in calcium compared with all other layers in the samples. In the 20°C samples the white layer shows a higher intensity than in either of the inner gray layers. This implies (1) that the calcium being dissolved in the gray layers, which contain unreacted cement phases (C-S-H and portlandite), is being deposited in the white layer and (2) that the calcium seen in the effluent-ICP data after the formation of the white layer is from its degradation.

5. Conclusions

At the pH and temperatures one might expect to find in a carbon sequestration site, a typical Class H well cement is subject to rapid degradation given the conditions of this experiment. The outer layers of the cements that were reacted at both pHs and both temperatures were fully degraded based on the results of the XRD and EPMA analyses. Although the formation of a calcium carbonate-rich layer, the white layer, retards the leaching of calcium from the cement, it does not stop it. Also, by the time the white layer forms, the dark gray core has already been reduced by about 2 mm in radius for each of the conditions presented here. The rate of degradation of the cement in these experiments after the formation of the white layer is controlled by the rate of dissolution of calcium carbonate, the white layer, and not diffusion through the brown or brown and orange layers.

Comparisons of the change in degradation rate between samples that were reacted at different pHs but at the same temperature and between samples that were reacted at different temperatures but at the same pH show that temperature has more of an influence on the rate of degradation than pH.

The most severe condition, influent pH 2.4 at 50°C, corresponds to the conditions of sequestration at 1 km depth in a sandstone formation and exhibits the most severe degradation. Although the other conditions were less severe and the progression of the degradation into the sample was slower the degradation was still significant.

It must be emphasized that these experiments set a severe upper bound on the rate of attack since the reaction in situ is most likely to occur under diffusion control, rather than reaction control. Detailed modeling is underway to evaluate the composition and flow rate of the brine that comes in contact with sealed wells at various distances from the point of injection.

References

- Andac, M., and Glasser, F. P., 1999, "Long-term leaching mechanisms of portland cement-stabilized municipal solid waste flyash in carbonated water," *Cement and concrete research*, Vol. 29, pp. 179-186.
- API, 1997, *API recommended practice 10B*. Washington D.C.: American Petroleum Institute.
- Brown, K., Jazrawi, W., Moberg, R., and Wilson, M., 2001, "Role of enhanced oil recovery in carbon sequestration. The Weyburn monitoring project, a case study," *Proceedings of the first national conference on carbon sequestration*.
- Bruant, R. G. Jr., Giammar, D. E., and Peters, C. A., Effects of pressure and solution composition on silicate dissolution rates as applied to geologic storage of carbon dioxide. In preparation (for *Geochimica et cosmochimica acta*).
- Bruckdorfer, R. A., 1986, "Carbon dioxide corrosion in oilwell cements," SPE 15176.
- Energy Information Administration, 2003, www.eia.doe.gov/emeu/iea/tableh1.html.
- Glasser, F., 1993, "Chemistry of cement solidified waste forms," in *Chemistry and microstructure of solidified waste forms*, edited by Spence, R., pp 1-39, Oak Ridge National Laboratory.
- Hitchon, B., 1996, *Aquifer disposal of carbon dioxide*. Sherwood Park, Alberta: Geoscience Publishing Ltd.
- Islam, M., Catalan, J., and Yanful, 2004, "A two-front leach model for cement-stabilized heavy metal waste," *Environmental science and technology*, Vol. 38, pp. 1522-1528.
- Onan, D. D., 1984, "Effects of supercritical carbon dioxide on well cements," SPE 12593.
- Smith, D. K., 1993 *Handbook on well plugging and abandonment*, Pennwell Books, Tulsa, Oklahoma.
- Statoil, 2000, "Carbon dioxide storage prized," <http://www.statoil.com/statoilcom/SVG00990.NSF?OpenDatabase&artid=01A5A730136900A3412569B90069E947>.
- Thaulow, N., Lee, R. J., and Sahu, S., 2001, "Effect of calcium hydroxide on the form, extent, and significance of carbonation," in *Calcium hydroxide in concrete*, edited by Skalny, J., Gebauer, J., and Odler, I., pp. 191-201, The American Ceramic Society, Westerville, Ohio.